ON THE BEHAVIOR OF THE PD/D SYSTEM: EVIDENCE FOR TRITIUM PRODUCTION

S. Szpak, P.A. Mosier–Boss,[1] and R.D. Boss
Naval Command, Control and Ocean Surveillance Center RDT & E Division San Diego, CA 92152 - 5000
and
J.J.Smith
Department of Energy, Washington, DC 20585

ABSTRACT

Evidence for tritium production in the *Pd*/*D* system under cathodic polarization is presented. A comparison of the observed distribution and that calculated, based upon the conservation of mass, leads to the conclusion that tritium is produced sporadically at an estimated rate of ca 10^3–10^4 atoms per second. The results of several runs are interpreted by employing the concept of an electrode/electrolyte interphase and the accepted kinetics of hydrogen evolution. Observation of burst-like events followed by longer periods of inactivity yield poor reproducibility when distributions are averaged over the total time of electrolysis.

1.0 INTRODUCTION

An early report on the behavior of the *Pd*/*D*- system, with atomic ratio [*D*]/[*Pd*] > 0.8, suggested that fusion of deuterium atoms occurs within the *Pd*- lattice when the system is under prolonged cathodic polarization(1). Among the observed behavior attributed to nuclear events, is the production of tritium which, for a number of reasons, appears to be an appropriate topic for investigation: First, a half century ago Oliphant *et al*.(2) reported that transmutation of deuterium into tritium and hydrogen occurs when a perdeutero inorganic compound, *e.g.*, $(ND_4)_2SO_4$, is bombarded with low energy deuterons. Second, a theoretical treatment concerning the occurrence of nuclear events when deuterium is electrochemically compressed in condensed matter indicate that tritium production can arise from *d-d* reaction in which the excited state of ^4He decays into $t + p$(3). Third, by simple mass balance arguments, low rate production of tritium has been reported by, among others(4), Will *et al.* (5) whose closed cell measurements make a compelling argument for excess tritium as a product of electrolysis. Finally, the analytical methods for the determination of tritium content are now well developed.

Below, we present data on tritium content and its distribution recorded in the course of electrolysis, in closed systems, of heavy water containing low level amounts of tritium. Our conclusions are based on the applicability of a model that was constructed before the present controversy evolved(6). In the course of charging the *Pd*- lattice with electrochemically generated deuterium, we have observed periods of detectable production of tritium. These periods occur sporadically and appear to be controlled, to a degree, by the structure of the interphase.

2.0 EXPERIMENTAL

The experimental procedure employed follows closely that described previously(7). Here, we provide a short summary of cell design and operation, analytical method for tritium analysis, including error estimates, and rationale for the manner in which the data are presented. We report data obtained from two sets of experiments, *viz.*, (i) electrolyte–gas phase tritium distribution recorded at about

[1]author to whom correspondence should be addressed.

24 hour intervals with intermittent electrolyte additions using an arbitrarily selected cell current profile and (ii) a three-phase distribution occurring within the time period required to reduce the initial volume of electrolyte by half at *a priori* selected constant cell current.

2.1 Electrolytic Cell; Current Profile

The electrochemical cell and recombiner are shown in Fig. 1. Each cell, with graduated wall to provide an additional check on the volume of electrolyte, was connected to a recombiner containing a catalyst (supplied by Ciner, Inc.) of sufficiently large surface area, (*ca* 100 cm^2), to assure nearly complete recombination of evolving gases. The working *Pd–* electrode was prepared as follows: *a ca* 3.0 cm^2 *Cu-* foil was wrapped around a glass rod, Fig. 1 – insert. Onto this foil a thin film of *Ag* was deposited from a cyanide bath. Although both metals act as an effective barrier for deuterium penetration, silver was added to provide a far better lattice match with the electrodeposited *Pd-* layer. The *Pd-* electrodes of two vastly different surface morphologies were prepared; one with a smooth surface by deposition from a $Pd(NH_3)2Cl_2 – H_2O$ solution at low current densities followed by drying prior to use, and the second with a mossy (dendritic) surface by electrodeposition from a $PdCl_2 – LiCl – D_2O$ solution in the presence of evolving deuterium. The placement of the counter electrode, made of a tightly coiled *Pt* wire, assured uniform current distribution on the working electrode. The cells were assembled in a dry box containing argon atmosphere.

The electrochemical charging of the *Pd-* electrodes was under galvanostatic control by a power source delivering constant current with 0.1 % ripple (EC & C Par model 363 potentiostat/galvanostat). The composition of electrolyte employed during charging is given in the respective figure captions. To increase the detection sensitivity, only heavy water with low tritium content, *ca* 19 *dpm/ml* (supplied by Isotec, Inc.), was used.

2.2 Sampling Procedure; Tritium Analysis

The sampling procedure is illustrated in Fig. 2. A known volume of electrolyte and tritium content, $V(t_1)$, is electrolyzed at a constant cell current, i, for a period of $\Delta t = t_2 – t_1$. During this time period the electrolyte volume is reduced by $Ve(t_2) = iM_w\Delta t/2\mathcal{F}\rho$. At time t_2, a sample is withdrawn, further reducing the electrolyte volume by V_s. Typically, immediately after sampling, the electrolyte volume is restored by addition of the electrolyte in the amount of $V_a(t_3) = 2V_s + V_e$. After a few minutes (to allow for mixing) a second sample, $V_s(t_4)$, is removed for tritium analysis. Removal of a second sample, following the electrolyte addition, assures that the electrolyte volume and tritium content are accurately known at the beginning of the next time interval. The sampling and addition procedures were carried out without the interruption of the cell current flow. Occasionally samples were removed without electrolyte addition.

Tritium content of the samples was measured by a liquid scintillation technique. In particular, 1 *ml* of sample is added to 10 *ml* of Fischer Scientific ScintiVerse E Universal LSC cocktail in a borosilicate vial. The prepared solutions were counted for 600 min in a Beckman LS 6000 LL scintillation counter. This instrument reports counts per minute (cpm) and disintegration per minute (dpm) with a 2σ error. To eliminate interference from chemiluminescence, all electrolyte samples were distilled to dryness and the distillate was analyzed for tritium content. Samples collected in the recombiner required no pretreatment.

The determination of the tritium content in the working *Pd-* electrode is a two-step procedure, namely the transfer of sorbed tritium into a liquid phase followed by scintillation counting. Two methods were employed to accomplish this transfer: (i) by anodic oxidation of sorbed tritium and

(ii) by the method described by Will *et al*. (5) involving the dissolution of the *Pd*- electrode in *aqua regia*. In the first case, the working electrode, while under cathodic overpotential, was rinsed by flushing the cell with $NaCl - H_2O$ solution to remove all D_2O containing tritium and placing it under the anodic overpotential of +0.5 *V vs Ag/AgCl* reference. In the second case, the *Pd*- electrode was dissolved in *aqua regia* and neutralized with $CaCO_3$. As with the electrolyte samples, the resultant solutions from both treatments were distilled to dryness, followed by scintillation counting of the distillate.

Error analysis included the assessment of the precision of measurements in (i) electrolyte volume, (ii) sampling/addition time intervals, (iii) constancy of cell current and (iv) tritium analysis. On the basis of an extensive investigation(7), we concluded that the largest error, as indicated by the instrument readout and determined by standard procedures, is in the tritium analysis. The typical error of 1.2 dpm is not the statistical error of counting but the cumulative uncertainty due to the propagation of error determined by a procedure commonly employed in the presentation of experimental data.

2.3 Intraphase Tritium Distribution

In the presentation of data and the subsequent analysis, we assume the validity of the model of the electrode-electrolyte interphase subject to restrictive conditions, of which one is the constancy of the isotopic separation factor. As shown in (7), the time dependence of tritium content in an open cell, operating galvanostatically with intermittent sampling, is given by Eq. (1)

$$f(t) = [m(0) - r(i)t]^{s-1}\left[\frac{f(0)}{m(0)^{s-1}} + \int_0^t \frac{q(t)}{[m(0) - r(i)t]^s}dt\right] \tag{1}$$

which, for $q(t) = const \neq 0$, we have Eq. (2)

$$f(t) = f(0)\left(\frac{m(0) - r(i)t}{m(0)}\right)^{s-1} + \frac{q}{(s-1)r(i)} \cdot \left\{1 - \left[\frac{m(0) - r(i)t}{m(0)}\right]^{s-1}\right\} \tag{2}$$

while, for $q(t) = 0$ it reduces to Eq. (3)

$$f(t) - f(0)\left(\frac{m(0) - r(i)t}{m(0)}\right)^{s-1} \tag{3}$$

where, f is the tritium mass fraction, m is the mass of the electrolyte phase, $r(i) = iM_w/2\mathcal{F}$ denotes the rate of change associated with the passage of cell current i, q is the rate at which tritium is added/removed from the solution phase by whatever process including transport of tritium generated in the bulk electrode, and s is the isotopic separation factor. The isotopic separation factor is defined here as $s - \left(\frac{C_T}{C_D}\right)_g / \left(\frac{C_T}{C_D}\right)_l$ and should be inverted to conform to values usually cited in the literature. A thorough discussion of the derivation of the above equations can be found in (7).

3.0 DISCUSSION

The long term electrolysis in open cells, with accompanying addition and removal of electrolyte, makes the determination of tritium production by total mass balance an unsuitable technique. This is especially true, should the tritium production be either low level or intermittent, due to the

propagation of error. We believe that a more appropriate procedure is based on the employment of the separation factor derived from the experimentally determined tritium content in both liquid and gaseous phases. Assuming that the Faraday law is obeyed, the ratio c_T/c_D in the gas phase is equal to the ratio of the corresponding faradaic currents, i_T/i_D, and tritium production is indicated by the difference between the calculated and observed data. In what follows, we examine the structure of the interphase, the origin and constancy of the isotopic separation factor and provide an interpretation of experimental data.

3.1 Structure of the Interphase; Transport Paths

The thermodynamic structure of the electrode/electrolyte interphase was formulated by van Ryssel-berghe(8). For the present purpose, we include the metal side and indicate only the relevant processes that influence the magnitude as well as the constancy of the isotopic separation factor, Figs. 3a – 3c. Irrespective of the operating rate determining step, species undergoing electroreduction, $c_m^{(r)}$; $m = D_2O, DTO$, are in equilibrium with those in the bulk (b) electrolyte, *i.e.*, $c_m^{(r)} \leftrightarrow c_m^{(b)}$. Superscript ($r$) refers to the location where the reactive species affect the rate through their electrochemical potentials, the r- plane, Fig. 3a. The reaction product, in an adsorbed state, $c_m^{(a)}$, is in equilibrium with those dissolved in the electrolyte, $c_m^{(b)}$, and when its solubility limit is exceeded, gas bubbles, which also are in equilibrium with the bulk electrolyte, are formed. The set of restrictive conditions that assures the constancy of the separation factor is: (i) evolution reaction of hydrogen isotopes is independent of each other, *i.e.*, $i = i_D + i_T$; (ii) sufficiently high overpotentials are applied so that the reverse reactions may be neglected; and (iii) system operates in a stationary state, *i.e.*, equilibria between various species are established resulting in $d\theta_m/dt = 0$(9). Under these conditions, the tritium distribution occurs *via* path **A** whereby the cell current i is divided into i_T and i_D and the hydrogen evolves from the electrolyte phase at the n- plane.

For the deuterium absorbing electrode material, the concept of the interphase must be extended to include the metal side as indicated in Figs, 3b and 3c by λ. If tritium is produced within the bulk electrode and transferred to the electrolyte phase, it must be first brought to the adsorption plane (a-plane). The constancy of the s- factor requires an equilibrium condition between species located within the interphase while the applicability of Eqs. (1) – (3) demands that all tritium bearing species first enter the electrolyte phase, *i.e.*, follow path **A**, Fig. 3b. The latter condition requires the presence of a charged ^nH; n = 1,2,3 species in the λ- layer that interacts with the OD^- ion. The existence of such species, *e.g.*, $[T \cdots T]^+$. $[D \cdots T]^+$, $[D \cdots D]^+$, was postulated in our recent publication(10). If, however, the conditions are such that transport to the electrolyte phase is prevented, path **B** becomes operative, resulting in substantial enrichment of the gas phase, Fig. 3c.

3.2 Evaluation of the separation factor

The reaction path for the evolution of hydrogen isotopes, H, D, T, is the same and is given by Eqs. (I) – (III),

$$H_2O^{(r)} + e^- \rightarrow H^{(a)} + OH^- \qquad \text{(I)}$$

followed by either

$$H_2O^{(r)} + H^{(a)} + e^- \rightarrow H_2^{(n)} + OH^- \qquad \text{(II)}$$

or

$$H^{(a)} + H^{(a)} \rightarrow H_2^{(n)} \qquad \text{(III)}$$

However, the reaction path for tritiated heavy water must be modified, *e.g.*, the controlling discharge step, Eq. (I), is split into two paths, Eqs. (IV) and (V)

$$DTO^{(r)} + e^{-} \rightarrow D^{(a)} + OT^{-} \tag{IV}$$

and

$$DTO^{(r)} + e^{-} \rightarrow T^{(a)} + OD^{-} \tag{V}$$

The same considerations apply when the rate determining step resides in either the Heyrovsky–Horiuti path, Eq. (II), or the Tafel path, Eq. (III).

A general form of an equation governing the charge transfer is

$$i_n = k_n c_n^{(r)} \cdot f(\theta_n) \cdot \exp(-\beta\eta \quad \not\# RT); \eta = E_{rev} - E(i); n = D, T \tag{4}$$

where the $f(\theta_n)$ function depends on the reaction path(9). Other symbols have their usual meaning. The atomic ratio in the gas phase, $(c_T/c_D)_g$, is the ratio of currents producing D_2 and DT, respectively. To obtain this ratio it is necessary to write Eq. (1) for both currents, *i.e.*, i_T and i_D and take a quotient, Eq. (5)

$$\left(\frac{c_T}{c_D}\right)_g = \frac{k_T c_T^{(r)} \cdot f(\theta_T)}{2k_D c_D^{(r)} \cdot f(\theta_D) + k_T c_T^{(r)} f(\theta_T)} \tag{5}$$

The factor of 2 in Eq. (5) appears because the D_2 molecules are produced by i_D and, on account of an equal probability of paths, Eqs (Ia) and (Ib), also include one half of those produced by i_T. For heavy water with low levels of tritium, $c_D >> c_T$ and, if the Volmer path is the rate determining step, then $f(\theta_n) = 1 - \theta_D - \theta_T$ is equal for both reactions, yielding the distribution in the gas phase, Eq. (6),

$$\left(\frac{c_T}{c_D}\right)_g = \frac{k_T c_T^{(r)}}{2 \cdot k_D c_D^{(r)}} \tag{6}$$

Theoretical considerations state that the isotopic separation factor is not affected by tritium concentration in the electrolyte, providing that $c_D >> c_T$(9). In writing Eqs. (5) and (6), we ignore the slight difference in the applied overpotential, *i.e.*, we assume that the difference in the rest potentials is insignificant.

3.3 INTERPRETATION OF DATA

In what follows, we provide a qualitative description of the tritium distribution as determined from the observed vs computed values of the D/Pd system under cathodic polarization. Following this, we supplement the description with a quantitative assessment; particularly, we select for discussion three aspects, *viz.*, assessment of observed behavior, data analysis and the rate of tritium generation and, finally, the location of tritium generating sites.

3.3.1 Qualitative Assessment

A qualitative assessment of tritium distribution between the electrolyte and gas phases resulting from a prolonged evolution of deuterium generated by the electrolysis of D_2O is given in Figs. 4–7. The electrolyses were carried out under varying cell current profiles and composition of additives. For convenience, changes in cell current, times of sampling and recombiner efficiency are indicated in respective figures (axes i, V_a and ε_r) while actual experimental data are provided in the appendix.

Three distinct scenarios can be seen from the data: (i) prolonged electrolysis without tritium production, (ii) sporadic tritium production with periods of inactivity wherein the isotopic separation factor is at or near the normal value for T/D systems throughout, and (iii) sporadic tritium production in which selective enhancement of the gas phase tritium level occurs. For all times in some cases, and for most time in all cases, there is good agreement between the calculated and observed tritium distribution, namely the experimental (solid line) and calculated (dashed line) fall within experimental error (shaded area). Those instances where significant deviation between the observed and expected concentration of tritium in both phases occurs indicates the periods of tritium production. In the figures, these regions are indicated by arrows, q_n; n = 1, 2, *3, 4.*

The first scenario: Tritium distributions summarized in Figs. 4a and 4b serve as examples of the absence of tritium production over the *ca* three weeks of duration of the electrolyses in solutions containing different additives, thereby also serving as blank tests of the model calculation for different charging profile. It is seen that the observed and calculated values are in good agreement.

The second scenario: In contrast, Figs. 5 and 6 show active periods of the type (ii) mentioned above. In Fig. 5, one active period of approximately three days duration, (6/21 – 6/23), occurs 30 days after the initiation of charging. Figure 6a shows two active periods, (4/19 – 5/3, 5/19 and 5/21), separated by 14 days of inactivity. In these instances the isotopic separation factor does not change and the enrichment occurs in both the electrolyte and gas phases. The constancy of the isotopic separation factor, $s = 0.68 \pm 0.04$, indicates that the reaction path for the cathodic charge transfer did not change, either in the course of prolonged electrolysis or between runs and, that tritium generated during the active periods first entered the electrolyte phase resulting in the isotopic distribution controlled by the electrodic reaction. Evidently, the distribution of tritium between the phases follows transport *via* route **A,** Fig. 3b, and the active period is therefore manifested by an increase in tritium concentration in both phases.

The third scenario: The data summarized in Fig. 7 show an active period in which tritium enrichment is limited to the gaseous phase only. This enrichment occurs shortly after the completion of the co–deposition process and is subsequently followed by a period of inactivity. The time dependent tritium concentration in the electrolyte agrees at all times with the computed values when $s = 0.67$. This selective enrichment of the gaseous phase suggests that path **B** is the method of transport. The return to a normal distribution indicates a transition from path **B** to path **A.** This behavior suggests that tritium production occurs shortly after completion of the co–deposition process and is affected by the morphology (mossy, dendritic) of the Pd- surface. The transition from path **B** to path **A** implies an active participation of the interphase region which, most likely, is attributed to the restructuring of the electrode surface as well to the enhanced concentration of hydrogen isotopes within the interphase region during the co–deposition process. A more detailed discussion of the dynamics of the interphase in the course of codeposition is outside the scope of this communication. A detailed presentation of the restructuring processes can be found in ref. (11).

We wish to remark that the absence of tritium production, Figs. 4a and 4b, means only that within the investigated period no activities were observed. It does not assure that they could not occur at some later date, a position expressed also by Bennington *et al*(12).

3.3.2 Data Analysis; Quantitative Aspects

The essential difference between the method employed here and elsewhere(4) concerns selection of the numerical value of the isotopic separation factor. This number is usually taken from the literature and may, or may not, represent the kinetic and thermodynamic properties of the interphase pertinent

to the experimental conditions. Here, the value of the *s*- factor is determined individually for each experimental run by selecting that value which best fits the recorded data.

In principle, the rate of tritium production is calculated by subtracting Eq. *(3)* from either Eq. (1) or Eq. (2). Taking as an example results plotted in Fig. 5, the difference between the observed and calculated tritium concentration in the electrolyte phase, on 6/22, is ca 4.0 dpm/ml. Tritium generation rates are estimated by a curve fitting technique(9) or by computer modeling in which an arbitrarily selected *q*- value is inserted into the experimental data and computer matched to obtain agreement with the observed distribution throughout the duration of the experiment. A good agreement was recorded for rate of tritium generation when $q = 610_3$ atoms/sec during period 6/21 – 6/22. This would indicate a total production of $5.2 \bullet 10^8$ tritium atoms.

An estimate of tritium production rate by a computer modeling technique is illustrated in Figs. 6a and 6b. In particular, the computed tritium distribution, with $q(t) = 0$, and data tabulated in Table A - I, is shown in Fig. 6a (solid circles) while the actual experimental distribution is shown by the open circles. Using the previous argument, we identify two periods of tritium production, the first occurring between 4/21 and 5/1 and the second starting on 5/18. The experiment was terminated on 5/21. The results of computer modeling based on tritium production: on 4/21 - *4/23* with $q_1 = 4 \bullet 10^3$ at/sec for $\Delta t = 3.016 \bullet 10^3$ min., on 5/18 with $q_2 = 3 \bullet 10^3$ at/sec. for $\Delta t = 1.442 \bullet 10^3$ min., on 5/19 with $q_3 = 7 \bullet 10^3$ at/sec for $\Delta t = 1.421 \bullet 10^3$ min., and on 5/20 with $q_4 = 3 \bullet 10^3$ at/sec for $\Delta t = 1.489 \bullet 10^3$ min. are shown in Fig. 6b. An excellent agreement with experimental distribution is evident with the total tritium production of $1.8 \bullet 10^9$ atoms.

The data shown in Fig. 7 provide the evidence for tritium production through the enrichment of the gas phase while retaining agreement between the computed and experimental point in the liquid phase. Unfortunately no estimate of the total amount of tritium production can be reliably made because of poor recombination efficiency. The poor efficiency means that the tritium content is, in reality, substantially higher than indicated (due to the faster rate of D_2/O_2 vs that of DT/O_2).

3.3.3 Tritium Generation Sites

The question of the location of the generation site for tritium production during the electrolysis of D_2O on a *Pd*- electrode cannot be resolved by the method just described. Data in Figs 5 – 7 were interpreted in terms of Eqs. (1) - *(3)* As written, these equations ignore the tritium absorption by the *Pd*- lattice and consequently, cannot provide any information concerning the location of the generating sites. However, this omission does not invalidate conclusions reached as long as $c_T << c_D$.

As in the earlier work of Will *et al.* (5), the resolution of this problem is sought by employing a total mass balance which, in addition, requires the determination of tritium content in the bulk of the Pd - electrode. The amount of tritium generated during several runs and its three-phase distribution is tabulated in Table I. This table lists the experimental conditions, columns 1 – 5, the distribution of tritium among the liquid, gas and bulk electrode, columns 6 - 8. A net increase in tritium content is indicated in columns 9 and 10 as either gain in *dpm* or in the number of tritium atoms produced in the course of an experiment. The latter is calculated by the method described above.

Data assembled in Table I are in general agreement with results obtained under conditions of intermittent sampling, Figs. 4 – 7. Three conclusions can be made, however: First, the long time between samplings obliterates the fine details of the behavior of the Pd/D system. For example, on the basis of the mass balance, rows 1, 2 and 4, no statement can be made concerning production of tritium or lack thereof, since the apparent change is much less than the analytical error and is,

therefore, not significantly different from no change. Second, tritium production, if any, takes place within, or in the close proximity of the interphase. Only when Al^{3+} ions were added to the electrolyte, was tritium detected in the bulk electrode. Third, electrolysis on dendritic surfaces (following the co–deposition) favors transport of tritium to the gas phase via path **B.**

4.0 Concluding Remarks

Because of the controversial nature of the Pd- lattice assisted nuclear events, we have refrained from speculations and concentrated on presentation and interpretation of experimental data. We have limited the discussion to one aspect only because the correlation with, for example, excess enthalpy production, would require an on-line detection system sensitive enough to record the low level activity. In conclusion, we emphasize the following points:

1. Every effort was made to minimize analytical errors in the closed system. Although closed cells are considered superior to closed system arrangements for the detection of tritium generation in electrolytic cells, a closed cell, by design, represents an integrating system which may not be desirable if you are ascertaining the nature of the tritium generation. In this communication, we have shown that the cell/recombiner assembly and our experimental protocols yield results identical with those obtained using closed cells. This is due to the fact that the greatest source of error in both experimental approaches is in the tritium content measurement itself and not in the electrolyte volume.

2. The evidence for tritium production is based on the difference between the computed and observed concentration of tritium, the non-equilibrium distribution of tritium and the total mass balance. Only accepted concepts and well established procedures lead us to the conclusions offered.

3. One of the characteristic features of the behavior of the Pd/D system is the sporadic nature of "burst-like" tritium generation. Short times between samplings are necessary to facilitate the display of the "burst-like" behavior. Such "burst-like" behavior would not be detectable using a closed cell system.

4. Present data indicate that tritium production takes place within the interphase with the distribution governed primarily by path **A.** A speculative argument can be presented to indicate that the generated tritium is forced into the bulk electrode by conditions at the solution side of the interphase, *e.g.* addition of Al^{3+} ions, and that electrode surface morphology tends to affect the two-phase distribution, e.g., dendritic surfaces tend to promote transport via path **B.**

ACKNOWLEDGEMENT

The authors acknowledge the interest and support received from Dr. Frank Cordon (NCCOSC – NISE West).

REFERENCES

1. M. Fleischmann and S. Pons, J. Electroanal. Chem., **261**, 301(1989)

2. M.L. Oliphant, P. Harteck and Lord Rutherford, Nature, **133**, 413 (1934)

3. J. Schwinger, **Nuclear Energy in Atomic Lattice,** The First Annual Conf. on Cold Fusion, p. 130, Salt Lake City, UT, 1990

4. E. Storms, Fusion Techn., **20,** 433 (1991)

5. F.G. Will, K. Cedzynska, M.—C. Yang, J.R. Peterson, H.E. Bergeson, S.C. Barrowers, W.J. West and D.C. Linton, **Studies of Electrolytic and Gas Phase Loading of Palladium with Deuterium,** The Science of Cold Fusion, Proc. II Annual Conf. on Cold Fusion, Como (Italy), 1991

6. R.V. Bucur and F. Bota, Electrochim. Acta, **29**, 103 (1984)

7. S. Szpak, P.A. Mosier-Boss, R.D. Boss and J.J. Smith, J. Electroanal. Chem., **373**, 1 (1994)

8. P. van Rysselberghe, Some Aspects of the Thermodynamic Structure of Electrochemistry, in Modern Aspects of Electrochemistry, J.O'M. Bockris, ed., vol. 4, Plenum Press, New York, NY , 1966

9. J. O'M. Bockris and S. Srinivasan, J. Electrochem. Soc., 111844(1964); 111,853(1964); **111,** 858 (1964)

10. S. Szpak, P.A. Mosier—Boss, S.R. Scharber and J.J. Smith, J. Electroanal. Chem., **337,** 147 (1992)

11. L. Schlapbach, **Surface properties and activation,** in Topics in Applied Physics, vol. II, chapter 2, Springer – Verlag, Berlin 1978

12. S.M. Bennington, R.S. Sokhi, P.R. Stonadge, D.K. Ross, M.J. Benham, T.D. Beynon, P. Whithey, I.R. Harris and J.P.G. Farr, Electrochim. Acta, 34,1323 (1989)

TABLE I: THREE PHASE TRITIUM DISTRIBUTION
(BY MASS BALANCE)

SYSTEMS	Volume/ml at			ϵ_r	Tritium/dpm/ml			$T = T(t_f) - T(t_o)$	
	t=0	$t=t_f$	T(l)/dpm/ml at t=0		Liquid	Gas	Electrode	dpm	atoms
Ag/0.3M LiCl	49.71	23.55	18.9±1.2	0.97	22.4±1.2	15.2±1.1	-	-14±50	
(Cu)Pd/0.1M LiOD	49.7	23.66	18.9±1.2	0.998	24.1±1.2	13.1±1.1	ND	-28±50	
(Ag)Pd/0.1M LiOD + 80ppm Al	49.72	29.49	18.0±1.2	1.00	25.4±1.2	13.3±1.1	2.3±1.3	123±50	5.1×10^{11}
(Ag)Pd/0.3M LiOD +231 ppm Al	49.69	19.79	16.5±1.2	0.97	20.3±1.2	13.1±1.1	0.9±1.3	-27±50	
(Au)Pd/0.3M LiCl[b] (co-dep)	46.72	11.8	14.5±1.9	0.56 (1.00)	25.4±2.1	13.4±1.8 (29.1)	ND[(a)]	90±80 (637)±80	2.6×10^{12}
(Au)Pd/0.3M LiCl[b] (co-dep)	37.1	16.1	17.0±1.9	0.50 (1.00)	25.1±2.1	13.4±1.8	ND[(a)]	60±60 (336)±60	1.3×10^{12}

(a) determined by method of Will et al (5).
ND - not detectable
(b) Sample were counted for 240 min instead of 600 min

FIGURE CAPTIONS

Fig. 1 - Experimental cell and recombiner assembly (schematic)
a — Electrolytic cell; **b —** Recombiner
insert - detail of cell assembly

Fig. 2 - Sampling profile for constant cell current density
$V(t_1)$ initial volume (also, initial volume for any charging period); $V(t2)$ – volume after the passage of charge $i\Delta t$; V_s - sample volume; V_a - volume added; t_2 - time of first sampling; t_3 - electrolyte addition time; t_4 - time of second sampling.

Fig. *3* - Structure of the interphase; tritium distribution paths
r - reaction site; a - adsorption site; e - charge transfer site; n - nucleation and gas evolution plane
3a - Fluxes on non-absorbing electrode: $i = i_D + i_T$ denote cell current and currents producing gaseous deuterium and tritium
3b - Fluxes on absorbing electrode - path **A**
3c - Fluxes on absorbing electrode - path **B**

Fig. 4 - Two-phase tritium distribution ($s = 0.71$)
computed - dashed; experimental - solid line
Fig. 4a - Electrode: area –3.67 cm^2; Cu-Ag-Pd (deposited from $Pd(NH_3)_2Cl_2$
Electrolyte: 0.01 M $PdCl_2$- 0.3 M LiCl – D_2O
Additive: 100 ppm $BeSO_4$ in 0.1 M $Li2SO_4$
Fig. 4b - Electrode: area – *3* cm^2*; Cu-Ag-Pd (* deposited from $Pd(NH_3)_2Cl_2$
Electrolyte: 0.3 M *LiOD*
Additive: 113 *ppm* B_2O_3
Cell current, electrode addition and recombining efficiency indicated by arrows along the time coordinate (i, V_a and ε_r respectively)

Fig. 5 - Two-phase tritium distribution ($s = 0.71$)
computed – dashed; experimental – solid lines
Electrode area: 2.5 cm^2; Cu-Ag-Pd deposited from $Pd(NH_3)_2Cl_2$
Electrolyte: $2.6 \bullet 10^{-3}$ M $PdCl_2$ – 0.31 M *LiCl*
Additive: 200 *ppm* $MgCl_2$
indicated: points of electrolyte addition; recombers efficiencies; cell current *(mA)*

Fig. 6 - Two-phase tritium distribution *(*$s = 0.63$)
Electrode area: 2.7 cm^2*; Cu-Ag-Pd* deposited from $Pd(NH_3)_2Cl_2$
Electrolyte: 0.33 M Li_2S0_4 (50 *ml)*
Additive: 100 *ppm* $BeS0_4$
indicated: cell current; recombining efficiency; electrolyte additions

Fig. 7 - Two-phase tritium distribution *(*$s = 0.67$)*
Electrode: prepared by co-deposition
Electrolyte: 0.05 M $PdCl_2$ + 0.6 M *LiCl*
indicated: cell current; recombiner efficiency; D_2O addition
*Note: the *s*- value computed using data of the last seven days

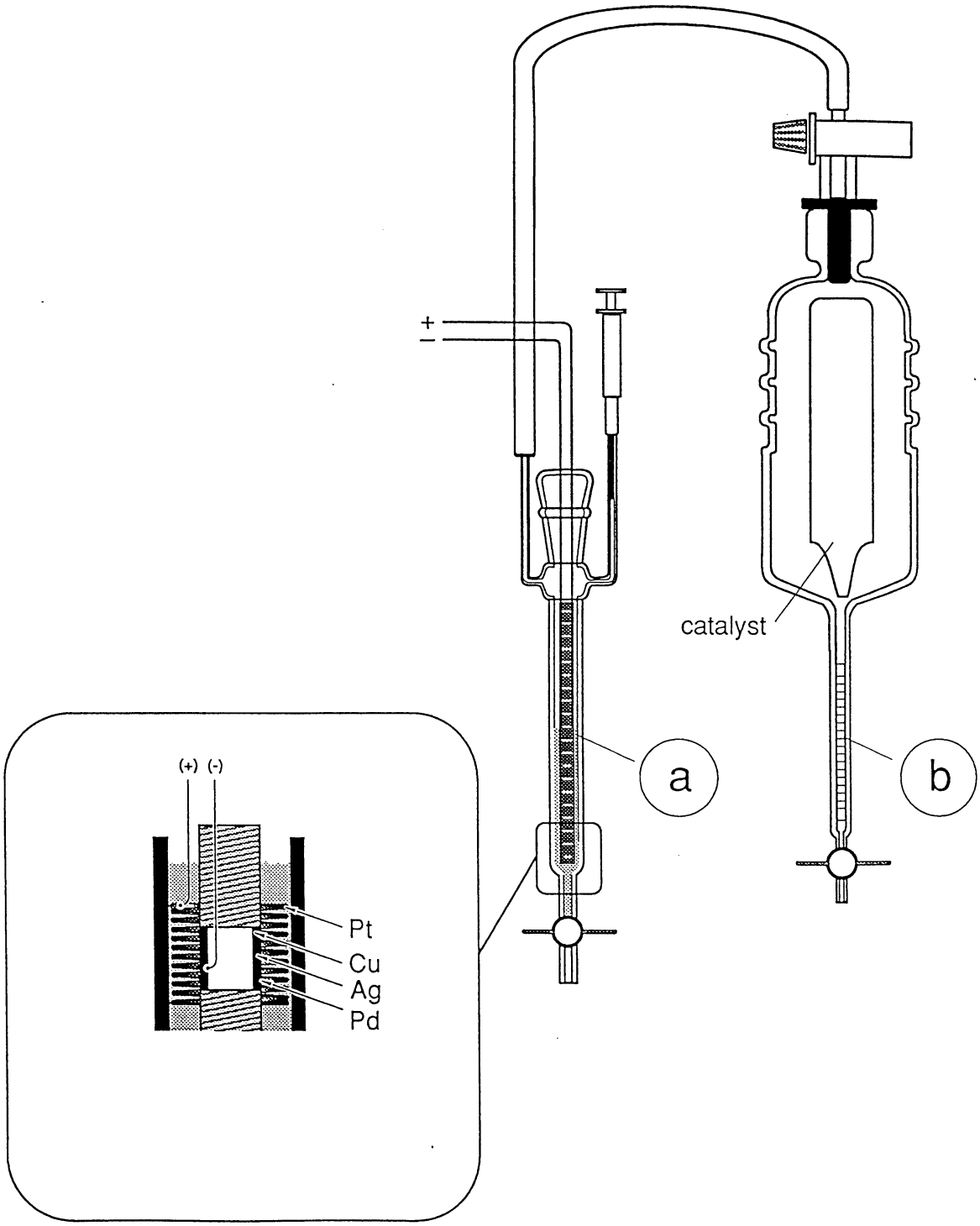
+
−
catalyst
a
b
(+) (-)
Pt
Cu
Ag
Pd

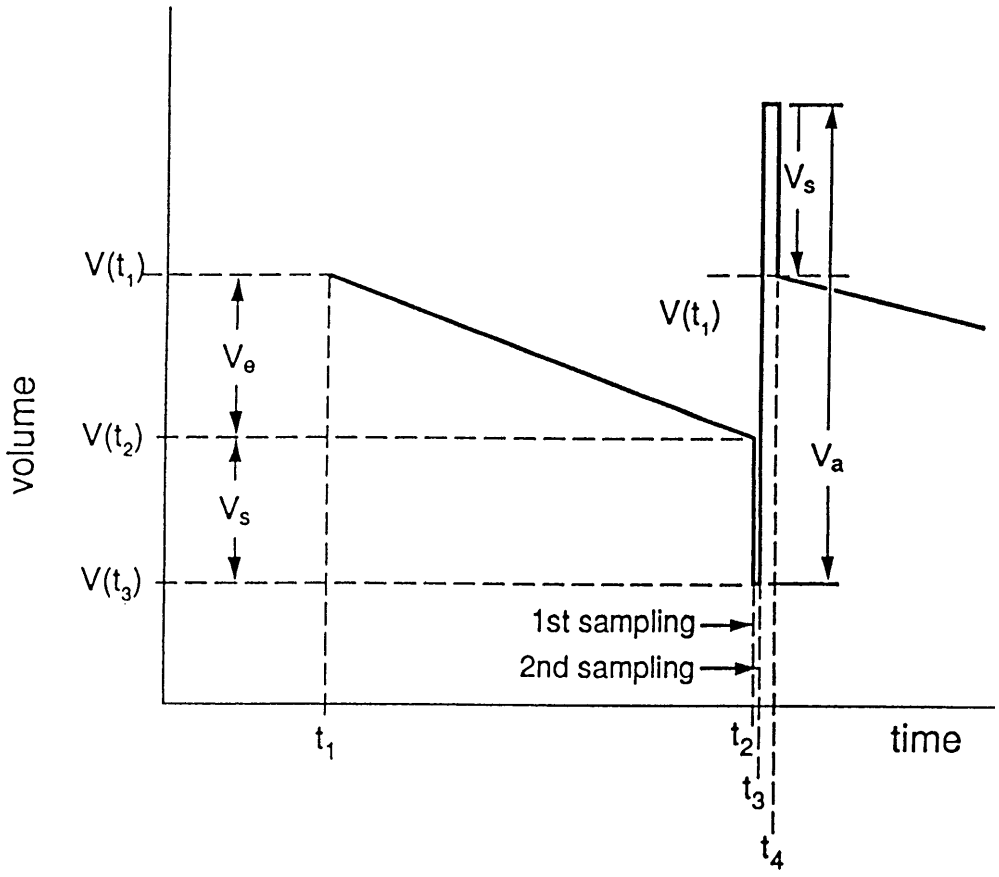
volume
V(t1)
Ve
V(t2)
Vs
V(t3)
Vs
V(t1)
Va
1st sampling
2nd sampling
t1
t2
t3
t4
time

a

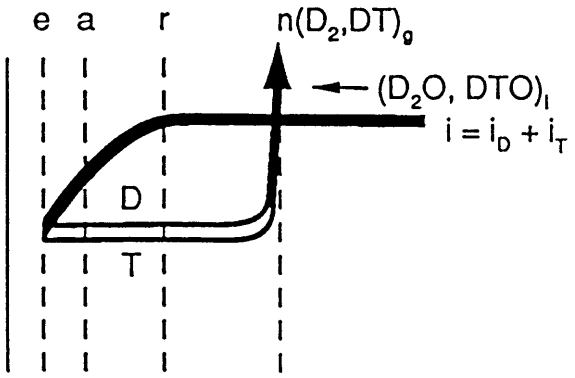
e a r
n(D2,DT)g
(D2O, DTO)l
i = iD + iT
D
T

b

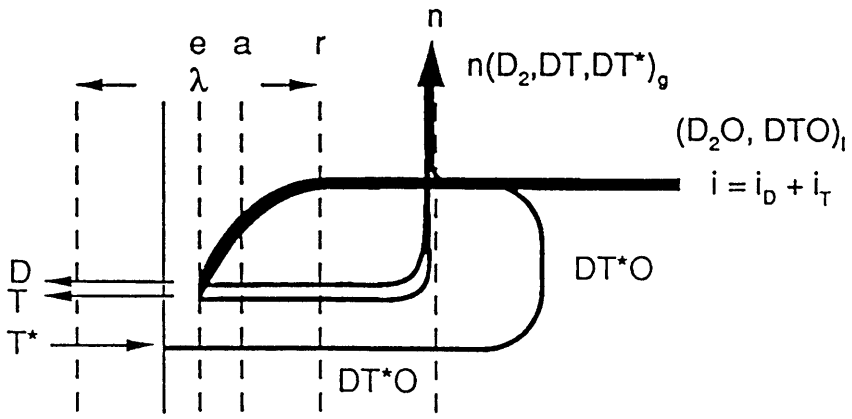
n
e a r
λ
n(D2,DT,DT*)g
(D2O, DTO)l
i = iD + iT
D
T
T*
DT*O
DT*O

c

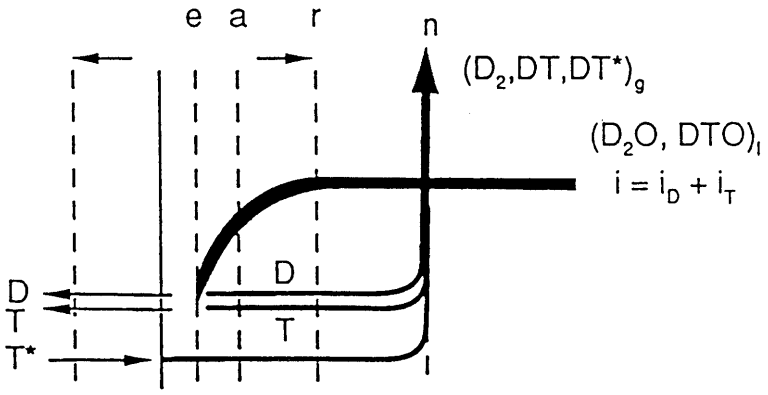
e a r
n
(D2,DT,DT*)g
(D2O, DTO)l
i = iD + iT
D
T
T*
D
T

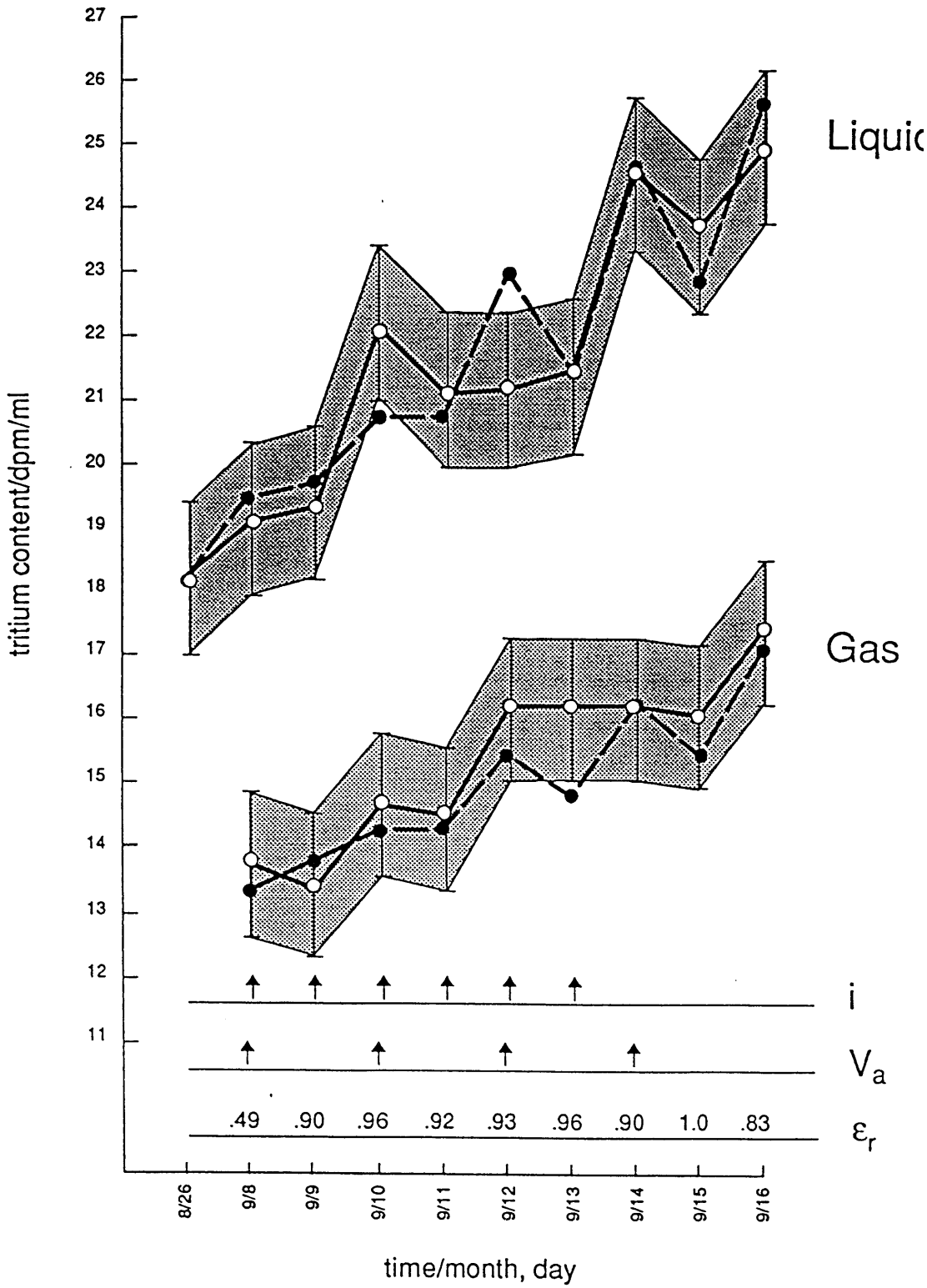
tritium content/dpm/ml
27
26
25
24
23
22
21
20
19
18
17
16
15
14
13
12
11
Liquic
Gas
i
V_a
.49 .90 .96 .92 .93 .96 .90 1.0 .83
ε_r
8/26 9/8 9/9 9/10 9/11 9/12 9/13 9/14 9/15 9/16
time/month, day

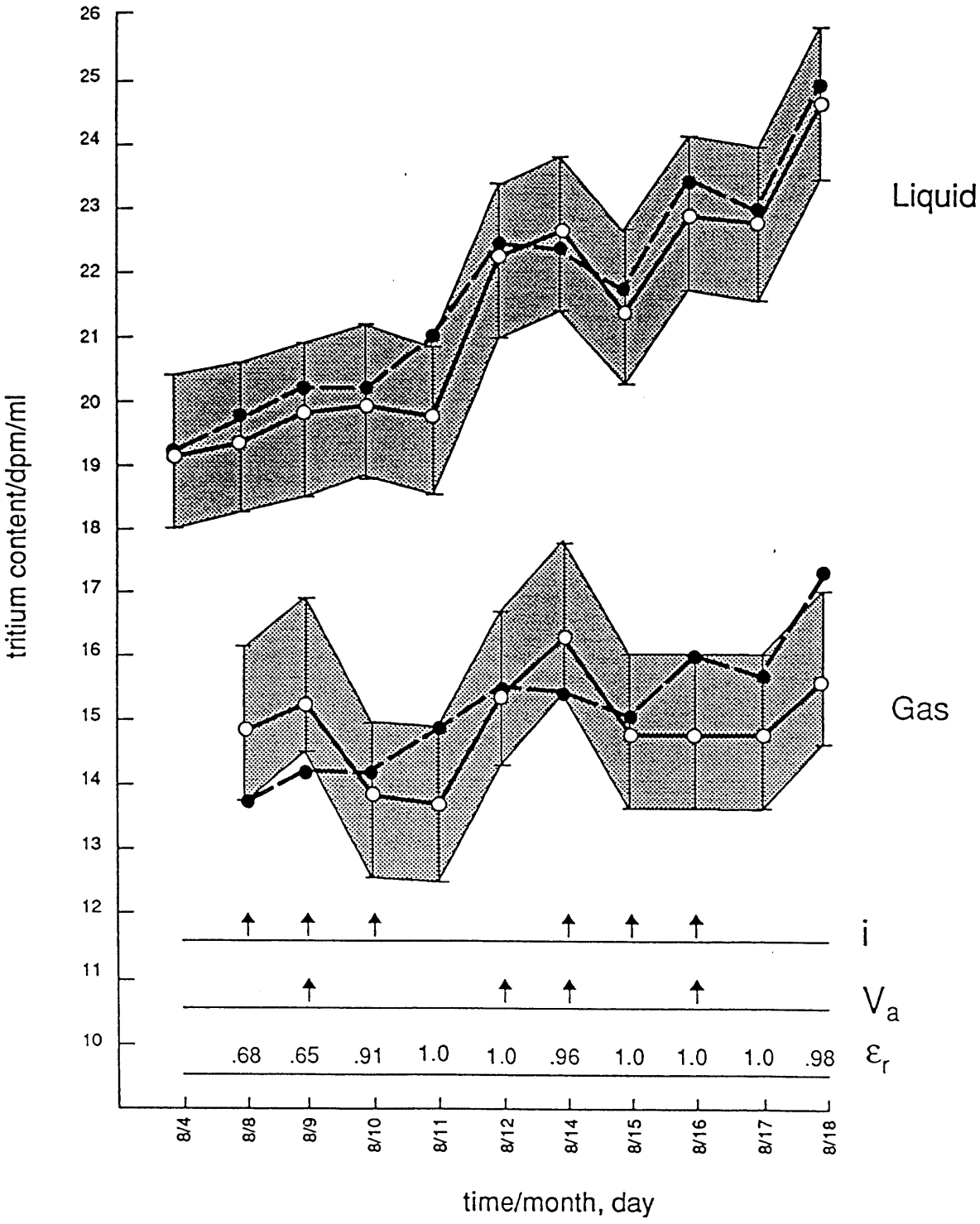
tritium content/dpm/ml
26
25
24
23
22
21
20
19
18
17
16
15
14
13
12
11
10
Liquid
Gas
i
V_a
ε_r
.68 .65 .91 1.0 1.0 .96 1.0 1.0 1.0 .98
8/4 8/8 8/9 8/10 8/11 8/12 8/14 8/15 8/16 8/17 8/18
time/month, day

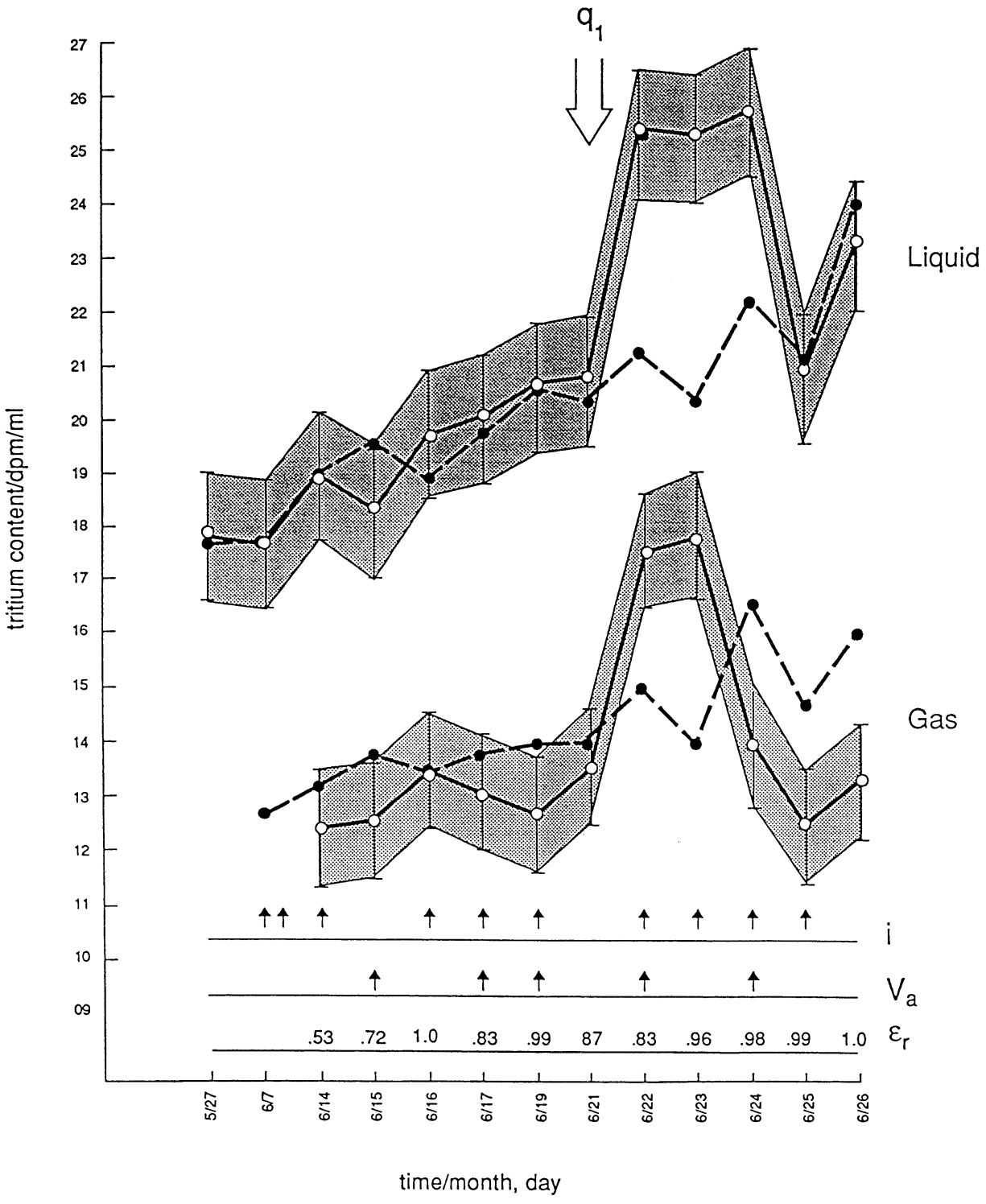
q_1
tritium content/dpm/ml
27
26
25
24
23
22
21
20
19
18
17
16
15
14
13
12
11
10
09
Liquid
Gas
i
V_a
ε_r
.53 .72 1.0 .83 .99 87 .83 .96 .98 .99 1.0
5/27 6/7 6/14 6/15 6/16 6/17 6/19 6/21 6/22 6/23 6/24 6/25 6/26
time/month, day

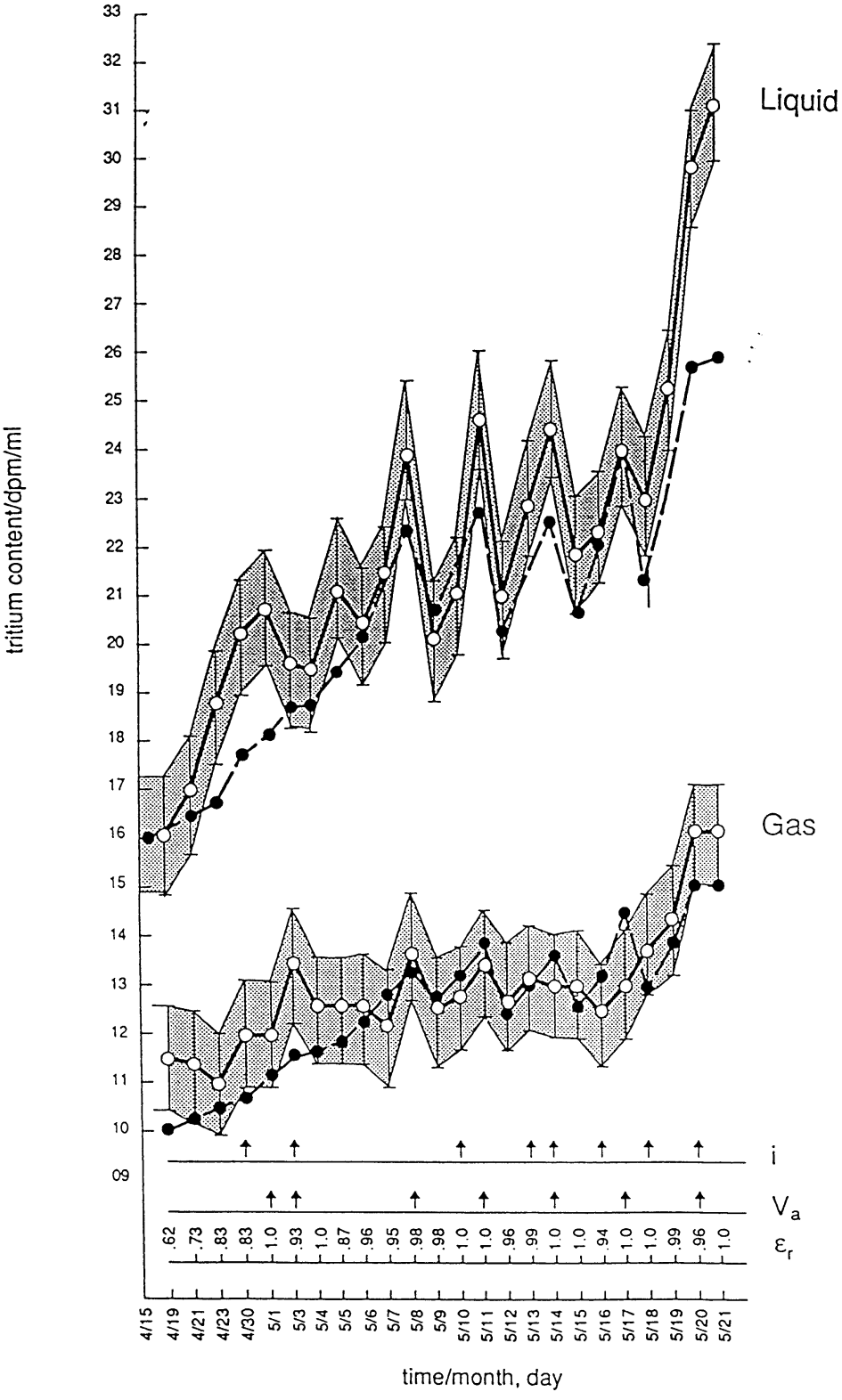
tritium content/dpm/ml
33
32
31
30
29
28
27
26
25
24
23
22
21
20
19
18
17
16
15
14
13
12
11
10
09
Liquid
Gas
i
V_a
ε_r
.62 .73 .83 .83 1.0 .93 1.0 .87 .96 .95 .98 .98 1.0 1.0 .96 .99 1.0 1.0 .94 1.0 1.0 .99 .96 1.0
4/15 4/19 4/21 4/23 4/30 5/1 5/3 5/4 5/5 5/6 5/7 5/8 5/9 5/10 5/11 5/12 5/13 5/14 5/15 5/16 5/17 5/18 5/19 5/20 5/21
time/month, day

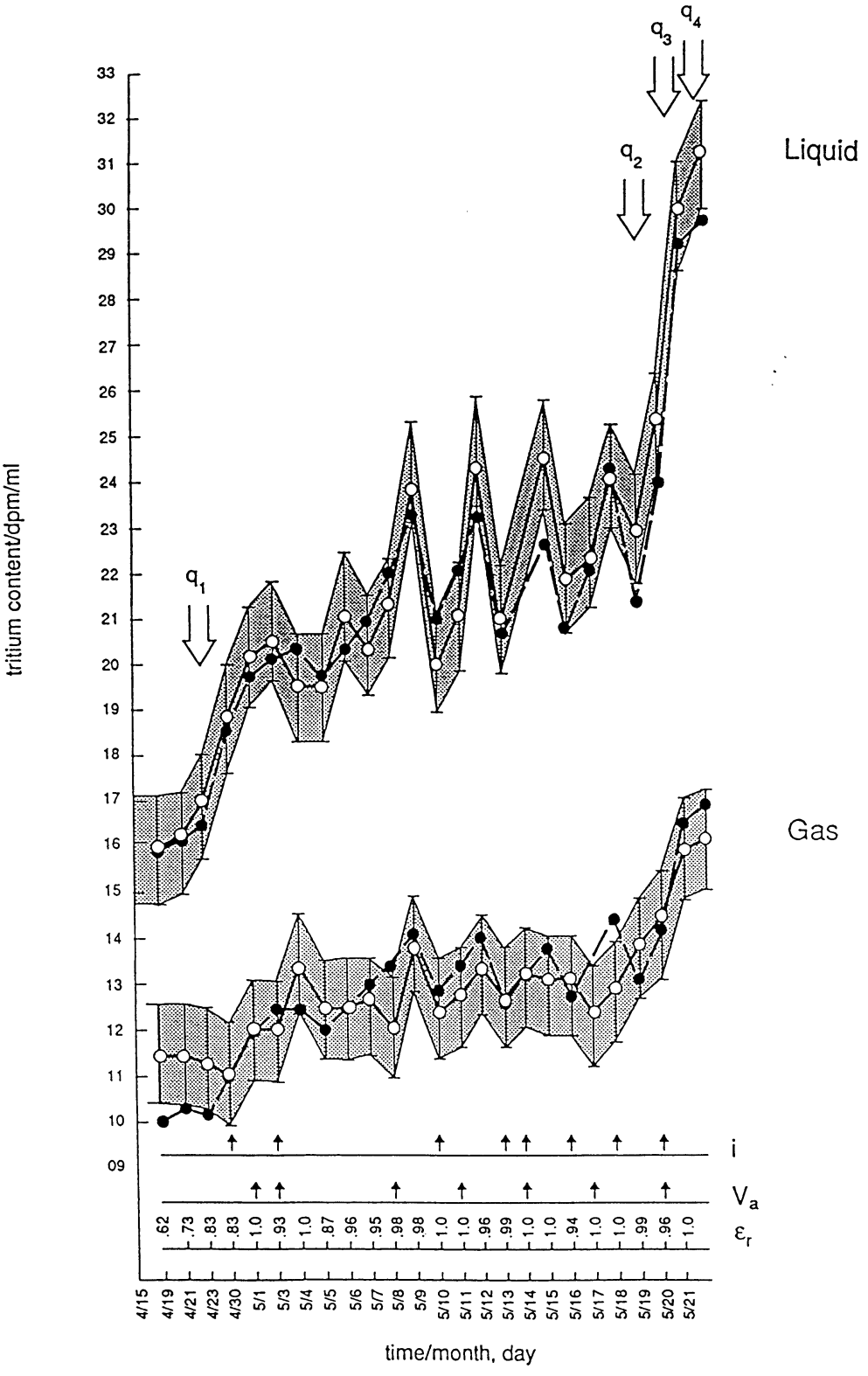
tritium content/dpm/ml
33
32
31
30
29
28
27
26
25
24
23
22
21
20
19
18
17
16
15
14
13
12
11
10
09
q_1
q_2
q_3
q_4
Liquid
Gas
i
V_a
ε_r
.62 .73 .83 .83 1.0 .93 1.0 .87 .96 .95 .98 .98 1.0 1.0 .96 .99 1.0 1.0 .94 1.0 1.0 .99 .96 1.0
4/15 4/19 4/21 4/23 4/30 5/1 5/3 5/4 5/5 5/6 5/7 5/8 5/9 5/10 5/11 5/12 5/13 5/14 5/15 5/16 5/17 5/18 5/19 5/20 5/21
time/month, day

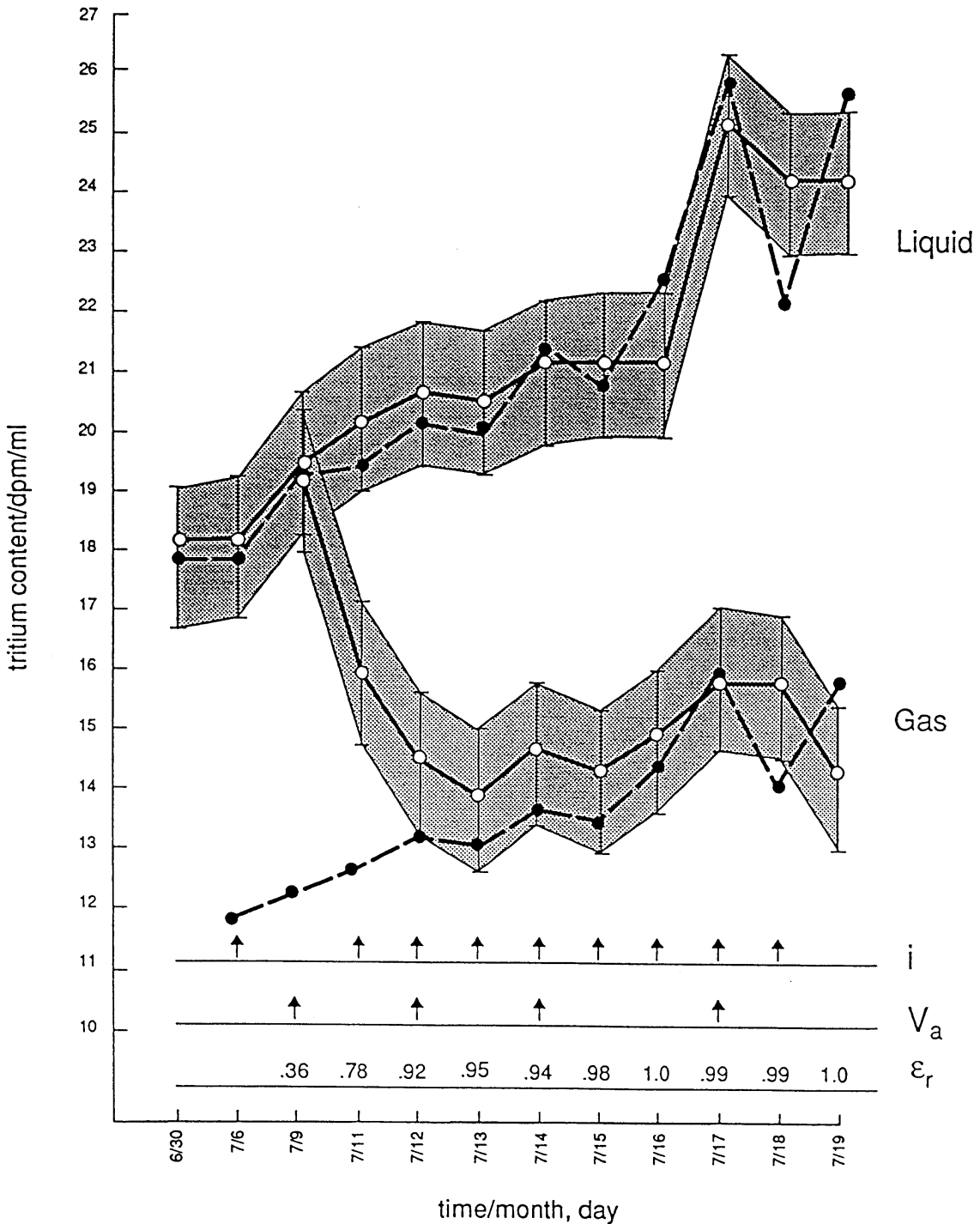
tritium content/dpm/ml
27
26
25
24
23
22
21
20
19
18
17
16
15
14
13
12
11
10
Liquid
Gas
i
V_a
ε_r
.36 .78 .92 .95 .94 .98 1.0 .99 .99 1.0
6/30 7/6 7/9 7/11 7/12 7/13 7/14 7/15 7/16 7/17 7/18 7/19
time/month, day

APPENDIX

Experimental data relevant to the computation of tritium distribution, using Eq. *(3)*, are tabulated in Tables A-I through A-V. They are assembled to supplement the information provided in the respective figure captions.

Table A-I: Inventory of Input Parameters for Figure 4a

Run: 26 Aug to 16 Sept 1993

Electrolyte - volume: 24.82±0.01 ml
- composition: 0.01 M $PdCl_2$ + 0.3 M LiCl in D_2O with T= 18.2±1.2 dpm/ml
- additions: (a) 0.1 M Li_2SO_4 + 102 ppm Be (as $BeSO_4$) in D_2O with T=18.2±1.2 dpm/ml (b) D_2O with T=18.2±1.2 dpm/ml

Separation factor s=0.71
Sampling volume V_s=1.60±0.01 ml

Sampling Date	i/mA	Δt/min	ϵ_r	V_s/ml	Tritium dpm/ml	
					Electrolyte	Gas
9-8	-5 -7.5 -100	1703 8280 8732	.49	9.08±0.02 [a]	19.2±1.2	13.8±1.1
9-9	-300	1463	.90		19.4±1.2	13.5±1.1
9-10	-500	1488	.96	15.14±0.02 [b]	22.3±1.2	14.8±1.2
9-11	-600	1768	.92		21.1±1.2	14.6±1.2
9-12	-800	1414	.93	18.17±0.02 [b]	21.2±1.2	14.5±1.2
9-13	-900	1076	.96		21.4±1.2	16.3±1.2
9-14	-1000	1626	.90	18.17±0.02 [b]	24.6±1.2	16.3±1.2
9-15	-1000	1449	1.00		23.6±1.2	16.2±1.2
9-16	-1000	1157	.83		25.0±1.2	17.4±1.2

Table A-II: Inventory of Input Parameters for Figure 4b

Run: 4 Aug 1993 to 18 Aug 1993

Electrolyte - volume 24.80±0.01 ml
- composition 0.3 M LiOD + 133 ppm B (as B_2O_3) in D_2O with T= 19.3±1.2 dpm/ml
- additions: 0.1 M LiOD + 50 ppm B in D_2O with T= 19.0±1.2 dpm/ml

Separation Factor s=0.71

Sampling volume V_s=1.60±0.01 ml

Sampling Date	i/mA	Δt/min	ϵ_r	V_a/ml	Tritium dpm/ml	
					Electrolyte	Gas
8-8	-50 -100	1421 4270	.68		19.4±1.2	15.0±1.2
8-9	-200	1738	.65	12.11±0.02	19.8±1.2	15.7±1.2
8-10	-300	1315	.91		20.0±1.2	13.8±1.2
8-11	-400	1442	1.00		19.7±1.2	13.6±1.2
8-12	-400	1593	1.00	12.11±0.02	22.2±1.2	15.5±1.2
8-14	-400	2460	.96	18.17±0.02	22.6±1.2	16.6±1.2
8-15	-600	1498	1.00		21.4±1.2	14.6±1.2
8-16	-800	1458	1.00	18.98±0.03	22.9±1.2	14.8±1.2
8-17	-1000	1668	1.00		20.3±1.2	14.8±1.2
8-18	-1000	1249	.98		24.6±1.2	15.8±1.2

TABLE III-A: Inventory of Input Parameters for Figure 5

Run: 27 May 1993 to 26 June 1993

Electrolyte - volume: 24.84±0.01 ml
- composition: 0.01M Pd Cl_2 + 0.314 M LiCl in D_2O with T=17.8±1.2 dpm/ml
- additions: 0.1 M LiCl + 200 ppm $MgCl_2$ in D_2O with T=17.0±1.2 dpm/ml

Separation factor s=0.71

Sampling volume V_s= 1.58±0.01 ml

Sampling Data	i/mA	Δt/min	ϵ_r	V_s /ml	Tritium	dpm/ml
					Electrolyte	Gas
6-7	-1 -2 -3	8612 1645 5546			17.7±1.2	
6-14	-50 -100	2947 7281	.53		18.9±1.2	12.4±1.1
6-15	-200	1496	.72	8.93±0.03	18.7±1.2	12.6±1.1
6-16	-200	1217	1.00		19.7±1.2	13.5±1.1
6-17	-300	1430	.83	8.93±0.03	20.0±1.2	13.1±1.1
6-19	-400	2801	.99	11.90±0.03	20.5±1.2	12.7±1.1
6-21	-300	3282	.87		20.7±1.2	13.6±1.1
6-22	-300	1435	. 83	11.90±0.03	25.3±1.2	17.6±1.1
6-23	-500	1411	.96		25.2±1.2	17.8±1.1
6-24	-600	1366	.98	17.87±0.03	25.7±1.2	13.9±1.1
6-25	-800	1211	.99		20.8±1.2	12.5±1.1
6-26	-1000	1363	1.00		23.3±1.2	13.3±1.1

Table IV-A: Inventory for Input Parameters for Figures 6a & 6b

Run: 15 Apr 1993 to 21 May 1993

Electrolyte - volume: 48.89±0.01 ml
- composition: 0.333 M Li_2SO_4 + 100 ppm Be (as $BeSO_4$) in D_2O with T=15.9±1.2 dpm/ml
- additions: (a) 0.1 M Li_2SO_4 in D_2O with T=15.9±1.2 dpm/ml
(b) 0.1 M Li_2SO_4 + 100 ppm Be (as $BeSO_4$) in D_2O with T=15 9±1.2 dpm/ml
(c) D_2O with T=16.0±1.2 dpm/ml

Separation factor: s=0.63
Sampling volume V_s= 2.06±0.01 ml

TABLE IV-A: FIGURES 6A AND 6B

Sampling Date	i/mA	Δt/min	ϵ_r	V_s /ml	Tritium dpm/ml	
					Electrolyte	Gas
4-19	-50 -100	1212 4286	.62		16.1±1.2	11.5±1.1
4-21	-100	2950	.73		16.9±1.2	11.4±1.1
4-23	-100	3016	.83		18.7±1.2	11.0±1.1
4-30	-100	9845	.83		20.2±1.2	12.0±1.1
5-1	-200	1424	1.00	8.94±0.01 [a]	20.8±1.2	12.0±1.1
5-3	-200	2977	. 93	20.85±0.02 [a]	19.4±1.2	13.5±1.1
5-4	-400	1470	1.00		19.4±1.2	12.5±1.1
5-5	-400	1325	.87		21.4±1.2	12.5±1.1
5-6	-400	1487	.96		20.4±1.2	12.6±1.1
5-7	-400	1524	.95		21.2±1.2	12.1±1.1
5-8	-400	1734	. 98	19.88±0.02 [a]	24.2±1.2	13.9±1.1
5-9	-400	1090	.98		20.1±1.2	12.5±1.1
5-10	-400	1667	1.00		21.0±1.2	12.8±1.1
5-11	-500	1396	1.00	23.83±0.02 [b]	24.8±1.2	13.5±1.1
5-12	-500	1305	. 96		20.9±1.2	12.8±1.1
5-13	-500	1551	. 99		23.0±1.2	13.2±1.1
5-14	-600	1194	1.00	25.34±0.02 [b]	24.6±1.2	13.0±1.1

5-15	-700	1450	1.00		21.8±1.2	13.0±1.1
5-16	-700	1543	.94		22.4±1.2	12.4±1.1
5-17	-800	1622	1.00	26.81±0.02 °	24.1±1.2	12.9±1.1
5-18	-800	1355	1.00		23.0±1.2	13.8±1.1
5-19	-900	1442	. 99		25.2±1.2	14.3±1.1
5-20	-900	1421	. 96	10.45±0.01 °	29.6±1.2	16.1±1.1
5-21	-1000	1489	1.00		31.2±1.2	16.1±1.1

Table A-V: Inventory of Input Parameters for Figure 7

Run: 30 June 1993 to 19 July 1993

Electrolyte - volume: 24.71±0.01 ml
- composition: 0.053 M $PdCl_2$ + 0.602 M LiCl in D_20 with T= 17.9±1.2 dpm/ml
- additions: D_20 with 17.9±1.2 dpm/ml

Separation factor s=0.67
Sampling volume V_s=1.58±0.01 ml

Sampling Date	i/mA	Δt/min	ϵ_r	V_s/ml	Tritium	dpm/ml
					Electrolyte	Gas
7-6	-0.5 -1 -2	1392 1432 5862			18.1±1.2	
7-9	-200	4227	.36	11.90±0.03	19.5±1.2	19.2±1.2
7-11	-200	2848	.78		20.4±1.2	15.9±1.2
7-12	-300	1476	.92	11.90±0.03	20.8±1.2	14.4±1.2
7-13	-400	1406	.95		20.6±1.2	13.8±1.1
7-14	-500	1515	.94	14.88±0.03	21.2±1.2	14.8±1.2
7-15	-600	1361	.98		21.3±1.2	14.2±1.2
7-16	-700	1421	1.00		21.3±1.2	14.9±1.2
7-17	-800	1329	.99	23.81±0.04	25.3±1.2	16.1±1.2
7-18	-900	1561	.99		24.4±1.2	15.9±1.2
7-19	-1000	1471	1.00		24.3±1.2	14.4±1.2